
Dynamic characterisation of a vehicle magnetorheological shock absorber

Zekeriya Parlak, Tahsin Engin*
and Şevki Çeşmeci

Department of Mechanical Engineering,
Sakarya University,
54187 Esentepe Campus, Sakarya, Turkey
E-mail: zparlak@sakarya.edu.tr
E-mail: engint@sakarya.edu.tr
E-mail: scesmeci@sakarya.edu.tr
*Corresponding author

İsmail Şahin

Vocational School of Akyazi,
Sakarya University,
Alagac Cad. Akyazi, 54405 Sakarya, Turkey
E-mail: isahin@sakarya.edu.tr

Abstract: Magnetorheological (MR) dampers have received remarkable attention due to being a potential technology to conduct semi-active control in mechanical systems in order to effectively suppress vibration. It is therefore important to understand the dynamic behaviour of such devices whose non-linear hysteresis is a complicated phenomenon. In the study, an MR damper has been designed, fabricated, tested and then its dynamic behaviour has been modelled with the classical Bouc-Wen hysteretic model. After that, the seven parameters of this model have been expressed in terms of only current excitation. By this, the total damping force has been given by a compact form in which the only independent variable is the current excitation. Finally, the model has been verified with experimental data and a good agreement has been observed.

Keywords: MR shock absorber; magnetorheological shock absorber; MR devices; MR fluid; MR damper; Bouc–Wen model.

Reference to this paper should be made as follows: Parlak, Z., Engin, T., Çeşmeci, Ş. and Şahin, İ. (2012) ‘Dynamic characterisation of a vehicle magnetorheological shock absorber’, *Int. J. Vehicle Design*, Vol. 59, Nos. 2/3, pp.129–146.

Biographical notes: Zekeriya Parlak was awarded his BS and MS in Mechanical Engineering from Trakya University and Sakarya University (Turkey) in 1998 and 2004, respectively. At present, he is a PhD Student at Sakarya University. His PhD research project has involved developing dynamic model and geometrical optimisation of a magnetorheological damper.

Tahsin Engin obtained his BS and MS in Mechanical Engineering from Hacetepe University and Karaelmas University (Turkey) in 1992 and 1995,

respectively, and his Doctorate in Mechanical Engineering from Sakarya University (Turkey) in 2000. Currently, he is an Associate Professor of Mechanical Engineering at Sakarya University, with research interests on tip clearance effects in centrifugal pumps and fans, solid–liquid flow through the pumps, hydraulic transportation of solids, thermal engineering optimisation, thermal and fluid flow considerations in process engineering, Newtonian and non-Newtonian fluid flows in microchannels, magnetorheological fluid flow considerations.

Şevki Çeşmeci received his BS and MS from Sakarya University, Turkey, in 2004 and 2007, respectively. And, he is currently pursuing a PhD on Magnetorheological Fluid Energy Absorbers at the University of Maryland, College Park, USA.

İsmail Şahin is an Assistant Professor of Vocational School of Akyazi at Sakarya University. He obtained his BS in Machine Teaching from Gazi University, his MS in Machine Teaching from Dumlupınar University and PhD in Machine Teaching from Sakarya University in 1993, 1996 and 2005, respectively. His research interests include magnetorheological dampers and applications, semi-active suspension systems, computer-aided designs and analysis and machine construction.

1 Introduction

Magnetorheological (MR) fluids are suspensions of magnetically polarisable particles with a few microns in size dispersed in a carrying liquid such as mineral or silicon oil. When a magnetic field is applied to the fluid, particles in the fluid form chains, and the suspension becomes like a semi-solid material due to increase in the apparent viscosity. Under the magnetic field, an MR fluid behaves as a non-Newtonian fluid with controllable viscosity. However, if the magnetic field is removed, the suspension turns out to be a Newtonian fluid in a few milliseconds, and the transition between these two phases is highly reversible, which provides unique feature of magnetic-field controllability of the flow of MR fluids. In general, an MR shock absorber consists of a hydraulic cylinder, magnetic coils and MR fluid. With no magnetic field, the MR shock absorber works in the fail-safe mode, i.e., as a classical passive dashpot. In addition to being field-controllable, MR shock absorbers have many advantages such that they

- require relatively very low power
- produce high-yield stress up to 100 kPa
- can be stably operated in a wide range of temperature (−40 to 150°C)
- are not toxic or sensitive against the impurities (Kim et al., 2009).

Owing to these advantages, MR shock absorbers have received great interest from different fields of applications including, but not limited to, automotive suspensions, seismic vibration mitigation, large bridges vibration control and knee prosthesis (Claudio and Donha, 2008).

Effective control of an MR shock absorber mainly depends on understanding of its non-linear hysteretic behaviour under an applied magnetic field. Therefore, one needs to develop control algorithms that take maximum advantage of unique features of the MR shock absorbers, and the models must adequately characterise intrinsic non-linear behaviour of the shock absorber (Spencer et al., 1997). The existing models can be classified into two categories, as parametric and non-parametric. Non-parametric models are able to model MR shock absorber behaviour in such a way that the model parameters do not necessarily have physical meanings (Boada et al., 2008). Some of the non-parametric models are Chebychev polynomials (Ehrgott and Masri, 1992; Gavin et al., 1996), Neural-Networks (Chang and Roschke, 1998; Chang and Zhou, 2002; Wang and Liao, 2004; Du et al., 2006) and Neuro-Fuzzy (Schurter and Roschke, 2000; Wilson and Abdullah, 2005). A literature survey would indicate that, although non-parametric models can effectively represent MR shock absorber behaviour, these are highly complicated and massive experimental data sets are necessitated for model validation.

Parametric models, on the other hand, are the most desirable ones, because their parameters have some physical meanings (Boada et al., 2008). These models consist of some mechanical elements such as linear viscous, friction element and spring. Parameters corresponding to these mechanical elements are determined on the basis of the experimental data. One of the first parametric models is the Bingham visco-plastic model developed by Stanway et al. (1987). In this model, a Coulomb friction element is placed in parallel with a linear viscous. Spencer et al. (1997) specified that the force–displacement behaviour appears to be reasonably modelled; however, this model does not exhibit the observed non-linear force–velocity response. A visco-elastic-plastic model based on Bingham visco-plastic model was proposed by Gamota and Filisko (1991). The model consists in adding a standard linear solid model in series with the original Bingham model. Wereley et al. (1998) proposed a non-linear hysteretic biviscous model. The model is an extension of the non-linear biviscous model having an improved representation of the pre-yield hysteresis. Wilson and Abdullah (2005) specified that the model could describe the force–displacement behaviour like other models, but in low velocity could not readily capture the force roll-off in force–velocity.

Non-linear hysteretic biviscous model was extended by Li et al. (2000), who reported that the deformation was visco-elastic in pre-yield region and visco-plastic in post-yield region. They also observed that the MR shock absorber operated post-yield rather than pre-yield region. Choi et al. (2001) proposed a polynomial model and compared the result of Bingham model and Bouc–Wen model, and showed that their model predicted fairly well the hysteresis behaviour under various conditions. Du et al. (2006) specified that polynomial model was a convenient and effective choice, which could realise the inverse dynamic of the MR shock absorber in an analytical form, and was easy to achieve the desirable shock absorber force in an open-loop control system. However, polynomial model cannot characterise the behaviour of the MR shock absorber favourably at relatively low-velocity region since this model does not include variables characterising the pre-yield property of the shock absorber force. Gavin et al. (2001) developed a hyperbolic tangent function to predict MR shock absorber force. They pointed out that the model did not have dynamic character and did not capture detail of frequency depending on visco-elastic behaviour, but algebraic model was corresponded to experimental results.

Most commonly used model for describing non-linear behaviour of MR shock absorbers is the Bouc–Wen model, which was initially proposed by Bouc early in 1971 and generalised by Wen (1976) and it has been known as the Bouc–Wen model since then. The model has been extensively chosen for its ability to capture, in a continuous function, a range of shapes of hysteresis loops, which resemble the properties of wide class of real non-linear hysteresis systems as stated by Dominguez et al. (2006) who developed a modified model based on their former studies. In their model, Bouc–Wen parameters were dependent not only on current excitation, but also on frequency and amplitude of the excitations. This model was able to predict the hysteresis force under any desired combination of current, frequency and amplitude of the excitations.

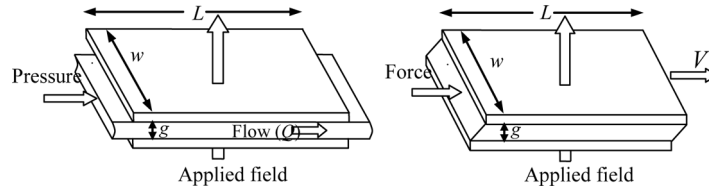
The general Bouc–Wen model predicts the force–displacement behaviour of the shock absorber well, and it possesses force–velocity behaviour that more closely resembles the experimental data. However, similar to the Bingham model, the non-linear force–velocity response of the Bouc–Wen model does not roll-off in the region where the acceleration and velocity have opposite signs and the magnitude of the velocities is small. Because of this reason, Spencer et al. (1997) proposed a modified Bouc–Wen model (phenomenological) to better predict the shock absorber response in this region. They estimated the parameters of modified Bouc–Wen model and compared the predicted responses against the corresponding experimental data. The proposed model predicted the behaviour of the shock absorber very well in all regions including in region where there are low velocities and the acceleration and velocity have opposite signs. Yang et al. (2001) proposed a modified model by taking the MR fluid inertial and shear thinning effects into account. Experimental verification of this Bouc–Wen-based model showed fairly good agreement with the experimental results. Dominguez et al. (2004) formulated a new model based on the Bouc–Wen model considering the current excitation as a variable to predict the force response of an MR shock absorber. The new methodology took into consideration the individual effect of each component of the Bouc–Wen model. Simulation results obtained using their methodology was validated with experimental data and results were in good agreement. However, some disagreements were reported between the proposed model and experimental data for low-current excitations.

In this paper, an experimental study and a dynamic modelling of a linear MR shock absorber has been carried out. To do this, a linear MR shock absorber has been designed, fabricated and tested. Then, the dynamic behaviour of the shock absorber was modelled by using analytical solution of simple Bouc–Wen model. The unknown coefficients in the model have been estimated by the parameter-optimisation technique. In the optimisation process, all parameters, except only one (i.e., n), have been assumed to be variable as opposed to what most of the authors did in the literature so far. It has been shown that the inclusion of all parameters could noticeably (by 3–9%) improve the accuracy of the modelling, which has crucial importance for a better control performance.

2 Design of the Magnetorheological (MR) fluid shock absorber

Most devices that use MR fluids can be classified as having either fixed poles (pressure-driven flow mode) or relatively moveable poles (direct-shear mode). Schematic for the two basic operational modes are given in Figure 1.

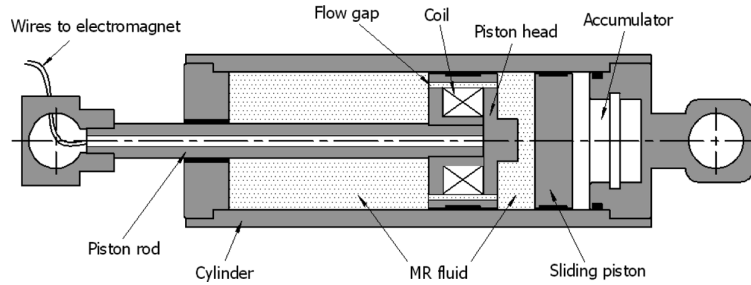
Figure 1 Basic operational modes for field-controllable fluid devices: (a) pressure-driven flow mode and (b) direct-shear mode



The hydraulic devices that use MR fluids, including shock absorbers, servo-valves, shock absorbers, are generally in pressure-driven flow mode, whereas MR brakes and clutches are in direct-shear mode.

Figure 2 shows a schematic for the prototyped MRD002 MR fluid shock absorber, which was designed and built at the University of Sakarya. The chambers that are separated by the piston head are filled with MR fluid, whereas the accumulator that is for compensating the volume changes induced by the movement of the piston rod to the up and down is filled with the pressurised nitrogen gas. During the motion of piston rod of the MR shock absorber, fluid flows through the annular gap opened on the piston head. Inside the piston head, a coil is wound around the bobbin shaft with a heat-resistant and electrically insulated wire. When electrical current is applied to the coil, a magnetic field develops around the piston head.

Figure 2 Schematic for the prototyped MR shock absorber



The magnetically induced iron particles inside the MR fluid line up in the direction of the magnetic flux lines to resist the flow producing a damping force. The mechanical energy that is required to yield this chain-like structure increases as the applied field increases resulting in a field-dependent yield stress. On the other hand, in the absence of a magnetic field, the MR fluid behaves like a Newtonian fluid. Therefore, the behaviour of MR fluid is often represented as Bingham plastic having a variable yield stress. The Bingham plastic model is given by

$$\tau = \tau_y(H) \operatorname{sgn}\left(\frac{du}{dr}\right) + \mu \frac{du}{dr} \quad |\tau| > |\tau_y| \quad (1)$$

$$\frac{du}{dr} = 0 \quad |\tau| < |\tau_y| \quad (2)$$

where τ is the shear stress, τ_y is the dynamic yield stress, H is the applied magnetic field intensity, du/dr is the shear strain rate and μ is the plastic viscosity of the MR fluid. However, true MR fluid behaviour exhibits some departures from Bingham plastic model. One and may be the most significant of these departures involves the non-Newtonian behaviour of the MR fluid in the presence of an applied field. Still, if used properly, equations (1) and (2) work well for the preliminary design of MR shock absorbers as well as other MR fluid devices.

The pressure drop across the flow channel of an MR valve is commonly assumed to result from the sum of viscous component ΔP_μ and a field-dependent induced yield stress component ΔP_τ and can be expressed as:

$$\Delta P = \Delta P_\mu + \Delta P_\tau = \frac{12\mu QL}{g^3 w} + \frac{c\tau_y L}{g} \quad (3)$$

where L , g and w are the length, gap and width of the flow channel between the stationary poles, respectively, Q is the volume flow rate through the channel, μ is the fluid viscosity with no applied field and τ_y is the yield stress developed in response to an applied field. The parameter c ranges from its minimum value of 2 (for $\Delta P_\tau / \Delta P_\mu$ less than ~ 1) to maximum value of 3 (for $\Delta P_\tau / \Delta P_\mu$ greater than ~ 100).

The volume of MR fluid exposed to the magnetic field and thus is responsible in providing the desired MR effect is named the minimum active volume V .

$$V = k \left(\frac{\mu}{\tau_y} \right) \lambda W_m \quad (4)$$

where k is a constant and $V = Lwg$ can be regarded as the necessary active volume to achieve the desired control ratio λ at a required controllable mechanical power level W_m . For pressure-driven flow: $k = 12/c^2$, $\lambda = \Delta P_\tau / \Delta P_\mu$ and $W_m = Q\Delta P_\tau$. By noting $V = Lwg$, equation (4) can be further manipulated to give

$$wg^2 = \frac{12}{c} \left(\frac{\mu}{\tau_y} \right) \lambda Q \quad (5)$$

Equation (5) provides geometric constraints and the aspect ratios needed for MR devices based on MR fluid properties, the desired control ratio and the device speed.

MR fluid devices are usually designed such that the MR fluid can be, or nearly can be, magnetically saturated so that the fluid will generate its maximum yield stress τ_y within a specified range. However, the value τ_y that is used in the above-mentioned equations should be chosen from the MR fluid specification sheets to reflect the anticipated operating condition.

The total force generated by an MR shock absorber consists of three components: Force due to the viscous effects F_μ , seal drag force (also friction force), which results from the relative motion between the mechanical components of the shock absorber F_f and field-dependent force F_τ which is actually a result of induced iron particles inside the MR fluid. These forces are schematically shown in Figure 3. The sum of the first two is referred as uncontrollable force since they generate a constant force according to any piston velocity, whereas the latter one is called controllable force, as it varies with the applied field. A dimensionless parameter, dynamic range D , which is defined as the ratio

of the total shock absorber force to the uncontrollable force, is introduced to evaluate the overall performance of an MR shock absorber:

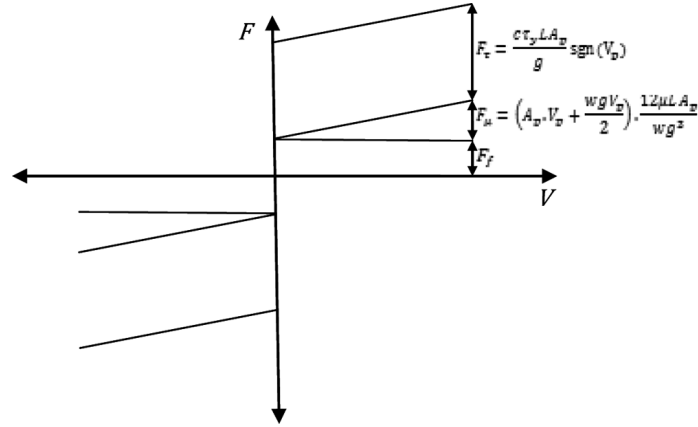
$$D = 1 + \frac{F_\tau}{F_\mu + F_f} \quad (6)$$

where

$$F_\mu = \left(A_p V_p + \frac{w_g V_p}{2} \right) \cdot \frac{12\mu L A_p}{w g^3} \quad (7)$$

$$F_\tau = \frac{c \tau_y L A_p}{g} \text{sgn}(V_p). \quad (8)$$

Figure 3 Force components of an MR shock absorber



The controllable force can be expanded to give:

$$F_\tau = \left(2 + \frac{12Q\mu}{12Q\mu + 0.4wg^2\tau_y} \right) \frac{\tau_y L A_p}{g} \text{sgn}(V_p) \quad (9)$$

which reveals that controllable force is inversely proportional to the gap size g . The dynamic ratio D is desired to be as large as possible to maximise the effectiveness of an MR shock absorber. One can think that this can be done simply by decreasing the gap size in equation (9). However, it is evident from equation (7) that decreasing the gap size below a critical value will decrease the dynamic range. The dynamic range, equation (6), can be rewritten as:

$$D = 1 + \frac{c \tau_y L A_p}{\left(A_p + \frac{w g}{2} \right) \frac{12 \mu L A_p V_p}{w g^2} + g F_f} \quad (10)$$

The second and may be the more important stage in the design considerations of an MR shock absorber is the magnetic circuit design, as a magnetic flux is required to induce

changes in the viscosity of the MR fluid. Although practical engineering notes can be found in the literature about the design procedure of the magnetic circuit, magnetic field developed around the piston head can also be analysed by finite element methods with the aid of commercial codes. It should be noted that an iterative calculus is needed between the flow geometry and magnetic circuit designs, which are coupled together especially through the flow gap g .

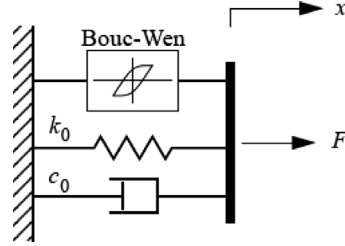
3 Modelling of hysteretic behaviour of MR shock absorber

3.1 Why need a dynamic hysteresis model?

Different models have been studied in the literature to describe the behaviour of MR shock absorbers. These models can be classified into two main categories as quasi-static flow models and dynamic models. While the quasi-static flow models can be successfully adapted to design MR shock absorbers, they unfortunately fail to capture the dynamic operational behaviour of these shock absorbers (Yang et al., 2001). That is, a quasi-static flow model such as Bingham plastic model can describe the force–displacement characteristic of an MR shock absorber effectively; however, it is not capable of describing the highly hysteretic force–velocity characteristic, which is, in fact, of crucial significance for a successful control performance of the shock absorber. Therefore, a dynamic hysteresis model is needed to simulate the hysteresis phenomenon of MR shock absorbers. To this end, various models have been proposed in the literature such as parametric viscoelastic-plastic model based on the Bingham model (Gamota and Filisko, 1991), the Bouc–Wen model (Dominguez et al., 2006), and many more. The Bouc–Wen model has offered the most accurate results of all, and thus has merited a special interest by the researches. Although it has been a powerful tool for characterisation of MR shock absorber behaviour, it has had drawbacks such as high computational costs in generating its characteristic parameters and has had accuracy problems. Over recent years, some efforts have been put to overcome such shortcomings and to enhance its success. One of the possible ways is first to solve the Bouc–Wen differential equation analytically, then to obtain the model parameters through a parameter-optimisation technique (Dominguez et al., 2006). The same procedure will also be applied in this study with the exception that all parameters will be taken to be variable in the optimisation process as opposed to previous studies. Therefore, it is expected that the inclusion of all parameters will enhance the accuracy of the modelling.

3.2 Current-dependent analytical solution of the Bouc–Wen model

The Bouc–Wen model, whose schematic is shown in Figure 4, is a numerically tractable dynamic model resembling both force–displacement and force–velocity behaviour of MR shock absorbers. The model essentially consists of a first-order non-linear differential equation that relates the input displacement to the output restoring force in a hysteretic way. It is possible to accommodate the response of the model to the real hysteresis loops by choosing a set of parameters appropriately.

Figure 4 Simple Bouc–Wen model


The total damping force in the Bouc–Wen can be expressed by Spencer et al. (1997) as follows:

$$f = c_0 \dot{x} + k_0 x + az \quad (11)$$

where z is the evolutionary variable and described by a first-order differential equation,

$$\dot{z} = -\gamma |\dot{x}| |z|^{(n-1)} z - \beta \dot{x} |z|^n + A \dot{x}. \quad (12)$$

The system of equations consists of seven characteristic parameters: α , β , γ , A , c_0 , k_0 and n . In equation (11), the first term ($c_0 \dot{x}$) represents the viscous force, the second term ($k_0 x$) reflects the linear force due to compressed gas in the accumulator and the last term (az) is the evolutionary force. Equation (12) can be expressed as follows:

$$\frac{dz}{dx} = A - ((\beta + \gamma \operatorname{sgn}(\dot{x}z))) |z|^n \quad (13)$$

where sgn represents the signum function. However, it has been revealed that the signs of z and \dot{x} are the same over the whole hysteresis loop. Therefore, the multiplication $\dot{x}z$ will always be positive and, thus, equation (13) can be rewritten as:

$$\frac{dz}{dx} = A - (\beta + \gamma) |z|^n \quad \text{for } z > 0; \dot{x} > 0 \text{ and } z < 0; \dot{x} < 0. \quad (14)$$

Solving equation (14) by setting $n = 2$ (Claudio and Donha, 2008; Yao et al., 2002) results in

$$z = \frac{\sqrt{A}}{(\sqrt{\beta + \gamma})} \tanh(\sqrt{A(\beta + \gamma)}(x + C)) \quad (15)$$

where C is the integration constant, which must be determined from the boundary condition. However, the boundary conditions to be imposed will be different for ($z > 0, \dot{x} > 0$) and ($z < 0, \dot{x} < 0$). To construct the hysteresis part due to the evolutionary variable (force–velocity behaviour), x should be replaced by \dot{x} in equation (15).

$$z = \sqrt{\frac{A}{\beta + \gamma}} \tanh(\sqrt{A(\beta + \gamma)}(\dot{x} + C)) \quad (16)$$

Equation (16) can be used to define the upper and lower hysteretic loops due to the evolutionary variable. The shape of the hysteretic curve can be described via different combinations of the parameters A , β and γ . By introducing equation (16), the evolutionary force $f_z = az$ can be rearranged to give

$$f_z = az = a \left[\sqrt{\frac{A}{\beta + \gamma}} \tanh \left(\sqrt{A(\beta + \gamma)} (\dot{x} + C) \right) \right]. \quad (17)$$

Solving for C by noting that $f_z = f_{z0}$ at $\dot{x} = 0$ yields

$$C = \frac{1}{\sqrt{A(\beta + \gamma)}} a \tanh \left(\frac{\pm f_{z0} \sqrt{\beta + \gamma}}{\alpha \sqrt{A}} \right) \quad (18)$$

where plus sign is for $z > 0$; $\dot{x} > 0$ and minus sign is for $z < 0$; $\dot{x} < 0$. Thus, equation (16) becomes

$$z = \sqrt{\frac{A}{\beta + \gamma}} \tanh \left(\sqrt{A(\beta + \gamma)} \left(\dot{x} + \frac{1}{\sqrt{A(\beta + \gamma)}} a \tanh \left(\frac{\pm f_{z0} \sqrt{\beta + \gamma}}{\alpha \sqrt{A}} \right) \right) \right). \quad (19)$$

Realising that $x = a \sin(\omega t)$ and $\dot{x} = a \omega \cos(\omega t)$, equation (11) becomes

$$f = c_0 (a \omega \cos(\omega t)) + k_0 (a \sin(\omega t)) + \alpha \left\{ \sqrt{\frac{A}{\beta + \gamma}} \tanh \left(\sqrt{A(\beta + \gamma)} \left(a \omega \cos(\omega t) + \frac{1}{\sqrt{A(\beta + \gamma)}} a \tanh \left(\frac{\pm f_{z0} \sqrt{\beta + \gamma}}{\alpha \sqrt{A}} \right) \right) \right) \right\} \quad (20)$$

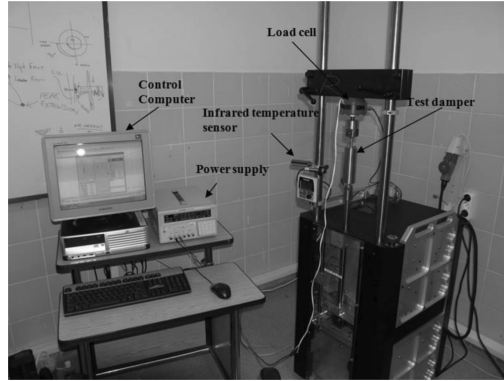
where a is the half stroke of the MR shock absorber and ω is the angular velocity of the piston head. As a result, the total damping force of the MR shock absorber has been expressed in a compact explicit form. The seven parameters α , β , γ , A , c_0 , k_0 and f_{z0} will be estimated via an optimisation technique by fitting the model equation to the experimental data.

4 Experimental study

The prototyped shock absorber, SAUMRD002, was tested on a mechanical scotch-yoke type shock machine of Roehrig Engineering Co. to obtain its characteristic curves as force vs. time, force vs. velocity and force vs. displacement. The experimental set-up is shown in Figure 5 with its main components. The shock machine has its own software to collect data from the data card and process them to plot force vs. time, force vs. displacement and force vs. velocity curves for each test. A programmable ‘‘GWinstek PPE 3223’’ power supply was used to feed current to the MR shock absorber. The machine has also an IR temperature sensor to read the temperature data during the tests. A load cell having a maximum capacity of 22 kN and a Linear Variable

Displacement Transducer (LVDT) was used to measure the damping force and displacement of the piston rod of the MR shock absorber, respectively. LVDT could also measure the relative velocity between the two ends of the shock absorber.

Figure 5 Experimental set-up with its main components



The shock absorber is fixed to the machine via grippers as shown in Figure 6. The dynamic tests of the prototyped shock absorber were performed under sinusoidal excitation at a range of 0–2 A, while maintaining the frequency and stroke at constant levels of 0.63 Hz and 12.5 mm, respectively.

5 Results and discussions

5.1 Model validation

In this study, the characteristic parameters α , β , γ , A , c_0 , k_0 and f_{c0} of an analytical expression derived based on the Bouc–Wen model were estimated for the prototyped MR shock absorber, SAUMRD002, employing a parameter-optimisation technique. Calculations were performed using the experimentally determined force–time curves of SAUMRD002 and the analytical expression given by equation (20).

Variation of the estimated parameters with the applied current, 0 A, 0.2 A, 0.4 A, 0.6 A, 1.0 A, 1.5 A and 2.0 A, excitation frequency of 0.63 Hz and half stroke of 12.5 mm is sketched in Figure 6.

It is seen from Figure 6 that the parameters β and γ have same values over the whole range of excitation current. This was also one of the alternative cases discussed by Wong et al. (1994). Further, they reported that the parameter A should increase as the excitation current increases, which are also the case for our particular study. It can be deduced from Figure 7 that all parameters tend to vary exponentially with the excitation current. Therefore, we proposed the model parameters to take the forms as follows:

$$c_0 I = c_{01} e^{c_{02} I} + c_{03} e^{c_{04} I} \quad (21a)$$

$$k_0 I = k_{01} + k_{02} (1 - e^{k_{03} I}) \quad (21b)$$

$$\alpha I = \alpha_1 + \alpha_2(1 - e^{\alpha_3 I}) \tag{21c}$$

$$\gamma(I) = \gamma_1 + \gamma_2(1 - e^{\gamma_3 I}) \tag{21d}$$

$$\beta I = \beta_1 + \beta_2(1 - e^{\beta_3 I}) \tag{21e}$$

$$AI = A_1 + A_2(1 - e^{A_3 I}) \tag{21f}$$

$$f_{z0}(I) = f_{z01}e^{f_{z02}I} + f_{z03}e^{f_{z04}I} \tag{21g}$$

where 23 constants were estimated based on the experimental data. The final forms of the seven parameters α , β , γ , A , c_0 , k_0 and f_{z0} in terms of excitation current and their corresponding correlation coefficients have been found to be as

$$c_0 I = 11510e^{-0.0349 I} + -8475e^{-1.029 I} \quad R^2 = 0.9823 \tag{22a}$$

$$k_0 I = 899.1 + 1810(1 - e^{-1.679 I}) \quad R^2 = 0.9686 \tag{22b}$$

$$\alpha I = 30.46 + 27.26(1 - e^{-0.9317 I}) \quad R^2 = 0.9923 \tag{22c}$$

$$\gamma I = 32.03 + -27.1(1 - e^{-3.916 I}) \quad R^2 = 0.9873 \tag{22d}$$

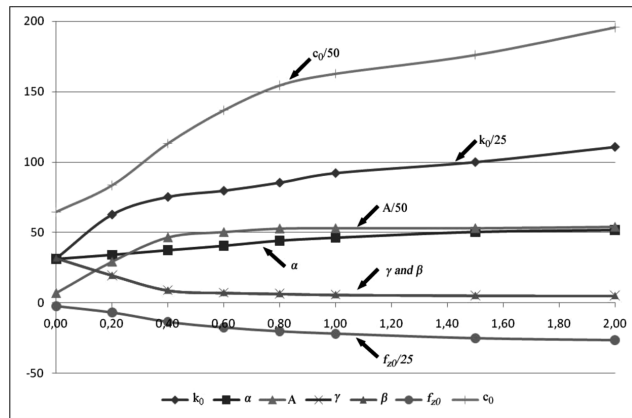
$$\beta(I) = 32.03 + -27.1(1 - e^{-3.916 I}) \quad R^2 = 0.9873 \tag{22e}$$

$$A(I) = 322.9 + 2389(1 - e^{-3.965 I}) \quad R^2 = 0.9914 \tag{22f}$$

$$f_{z0}(I) = -1214e^{-0.1912 I} + 1175 e^{-0.9509 I} \quad R^2 = 0.9948. \tag{22g}$$

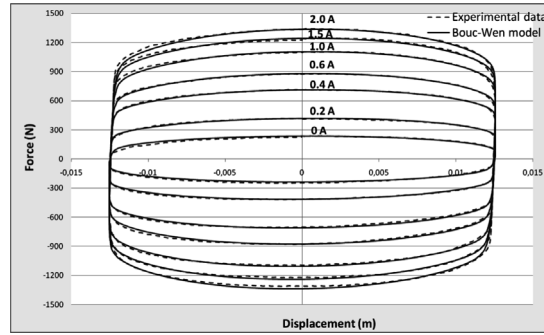
It is realised from correlation coefficients that the proposed forms of parameters can successfully represent the general trend of the variation of parameters against excitation current.

Figure 6 Parameters $c_0, k_0, a, A, \gamma, \beta, f_{z0}$ vs. current excitations

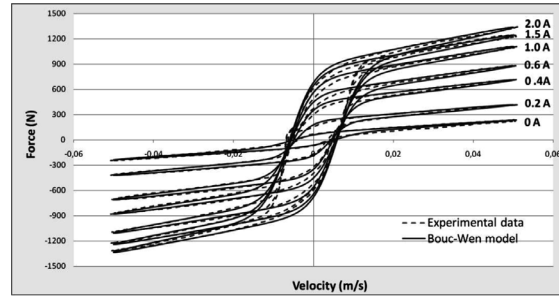


Comparisons between the model results and experimental data for each excitation current are given in Figure 7.

Figure 7 Comparisons between the model results and experimental data for excitation currents of 0 A, 0.2 A, 0.4 A, 0.6 A, 1.0 A, 1.5 A and 2.0 A, excitation frequency of 0.63 Hz and half stroke of 12.5 mm: (a) force–displacement and (b) force–velocity



(a)



(b)

As can be seen from Figure 7, the increase in damping force is more prominent at lower excitation currents, i.e., 0–0.6 A. However, this increase decays gradually at higher excitation currents, i.e., 1.0–2.0 A, which can be attributed to the fact that MR shock absorber is magnetically saturated with increasing excitation current.

It is observed that there is a good agreement between the results obtained from the Bouc–Wen model and experimental data. It can be deduced from Figure 7(b) that the model can characterise the hysteresis behaviour of the MR shock absorber in very good agreement. In addition to the graphical evidence, a quantitative error analysis will be carried out.

5.2 Error analysis

The error analysis between the predicted force obtained from the model and experimentally measured force has been done as a function of time, displacement and velocity, which was given by Spencer et al. (1997) as

$$E_t = \sqrt{\frac{\int_0^T (F_{\text{exp}} - F_{\text{mod}})^2 dt}{\int_0^T (F_{\text{exp}} - \mu_{\text{exp}})^2 dt}} \quad (23)$$

$$E_x = \sqrt{\frac{\int_0^T (F_{\text{exp}} - F_{\text{mod}})^2 \left| \frac{dx}{dt} \right| dt}{\int_0^T (F_{\text{exp}} - \mu_{\text{exp}})^2 dt}} \quad (24)$$

$$E_x = \sqrt{\frac{\int_0^T (F_{\text{exp}} - F_{\text{mod}})^2 \left| \frac{dx}{dt} \right| dt}{\int_0^T (F_{\text{exp}} - \mu_{\text{exp}})^2 dt}} \quad (25)$$

where F_{exp} is the experimental force, F_{mod} is the predicted force calculated by equation (20) and μ_{exp} is the mean value of experimental force during one cycle of the MR shock absorber. The results of the error analysis for each excitation current are tabulated in Table 1.

Table 1 Results of error analysis of MR shock absorber model

Current (A)	E_t	E_x	$E_{\dot{x}}$
0	0.0711	0.0097	0.0276
0.2	0.0238	0.0027	0.0095
0.4	0.0228	0.0026	0.0093
0.6	0.0248	0.0027	0.0103
1.0	0.0278	0.0030	0.0116
1.5	0.0295	0.0032	0.012
2.0	0.0294	0.0032	0.0122

To better reveal the success of the model studied here, we also estimated the parameters by using the model suggested by Dominguez et al. (2006) and a model obtained by adding an inertial term to this model, which was first suggested by Yang et al. (2001), for the same experimental data. Dominguez et al. (2006) proposed a model based on the Bouc-Wen model, where they assumed that the parameters n , β , and A are constants. The errors associated with these two models are listed in Tables 2 and 3.

Table 2 Results of error analysis for the model suggested by Dominguez et al.

Current (A)	E_t	E_x	$E_{\dot{x}}$
0	0.0551	0.0076	0.0209
0.2	0.0321	0.0030	0.0133
0.4	0.0286	0.0030	0.0119
0.6	0.0300	0.0031	0.0128
1.0	0.0329	0.0035	0.0140
1.5	0.0340	0.0039	0.0142
2.0	0.0347	0.0039	0.0145

Source: Dominguez et al. (2006)

Table 3 Results of error analysis for the model modified with an inertial term based on Yang et al. (2001)

Current (A)	E_t	E_x	$E_{\dot{x}}$
0	0.0459	0.0067	0.0169
0.2	0.0309	0.0032	0.0127
0.4	0.0276	0.0030	0.0114
0.6	0.0311	0.0032	0.0132
1.0	0.0339	0.0036	0.0142
1.5	0.0354	0.0039	0.0146
2.0	0.0336	0.0035	0.0140

A detailed examination of Tables 2 and 3 reveals that our model is more successful than the both models by about 3–9%.

Substituting equation (21) into equation (20) results in equation (26), which is only a function of excitation current. Calculations have been repeated for equation (26) and corresponding errors are listed in Table 4.

$$\begin{aligned}
 f = & (c_{01}e^{c_{02}t} + c_{02}e^{c_{04}t})(a\omega\cos(\omega t)) + (k_{01} + k_{02}(1 - e^{k_{02}t}))(a\sin(\omega t)) \\
 & + (a_1 + a_2(1 - e^{a_2t})) \\
 & \left\{ \frac{(A_1 + A_2(1 - e^{A_2t}))}{\sqrt{(\beta_1 + \beta_2(1 - e^{\beta_2t})) + (\gamma_1 + \gamma_2(1 - e^{\gamma_2t}))}} \right. \\
 & \left. \tanh\left(\sqrt{(A_1 + A_2(1 - e^{A_2t}))(\beta_1 + \beta_2(1 - e^{\beta_2t})) + (\gamma_1 + \gamma_2(1 - e^{\gamma_2t}))}\right) \right. \\
 & \left. \left(a\omega\cos(\omega t) + \frac{1}{\sqrt{(A_1 + A_2(1 - e^{A_2t}))(\beta_1 + \beta_2(1 - e^{\beta_2t})) + (\gamma_1 + \gamma_2(1 - e^{\gamma_2t}))}} \right) \right. \\
 & \left. \left. a \tanh\left(\frac{\pm(f_{z01}e^{f_{z02}t} + f_{z02}e^{f_{z04}t})\sqrt{((\beta_1 + \beta_2(1 - e^{\beta_2t})) + (\gamma_1 + \gamma_2(1 - e^{\gamma_2t}))}})}{(\alpha_1 + \alpha_2(1 - e^{\alpha_2t}))\sqrt{(A_1 + A_2(1 - e^{A_2t}))}}\right) \right) \right\}. \tag{26}
 \end{aligned}$$

Table 4 Results of error analysis for the model given by equation (26)

Current (A)	E_t	E_x	$E_{\dot{x}}$
0	0.1591	0.0147	0.0615
0.2	0.1581	0.0209	0.0577
0.4	0.0989	0.0126	0.0338
0.6	0.0564	0.0055	0.0171
1.0	0.0524	0.0047	0.0189
1.5	0.1022	0.0091	0.0371
2.0	0.1215	0.0092	0.0478

The comparisons show that equation (23) can be satisfactorily employed to simulate the hysteretic behaviour of the MR shock absorber. The higher errors E_t , E_x and $E_{\dot{x}}$ of equation (23) compared with that of equation (20) is due to the fact that the model parameters were estimated approximately through a parameter-optimisation technique in their proposed forms. The associated correlation coefficients were given in equation (22). Equation (23) is more preferable over equation (20) in the sense that it is only current dependent and, thus, one can estimate the model parameters by only changing the excitation current.

6 Conclusions

In this study, an MR shock absorber model suggested by Dominguez et al. (2006) is employed in a different fashion such that all model parameters were assumed to be variable except n , unlike as in the original model where three model parameters n , β and A were supposed to be constant. Then, the model results were compared with the experimental data to validate the model. To do this, an MR shock absorber, MRD002, was designed, fabricated and tested at the Applied Fluid Mechanics Laboratory (AFML), Sakarya University. The comparisons showed that there was a good agreement between the model results and experimental data. Furthermore, we compared our model against a prior model suggested by Dominguez et al. (2006) and a model obtained by modifying this model by adding an inertial term, which was first suggested by Yang et al. (2001), through an error analysis to better reveal the success of our model. Comparisons of error analysis of each model proved that our model was more successful than the other models by about 3–9%.

Also, we modified the model equation, equation (20), by substituting the model parameters in the proposed forms so as to generate an equation that is only current dependent. The resulting equation, equation (26), was then employed to estimate the model parameters for each excitation current. The error analysis of the model given by equation (26) revealed that the model was not as successful as the model given by equation (20). However, equation (26) can still be used successfully owing to its simplicity and practicality to develop more effective control algorithms as it depends on only one parameter (current excitation) rather than seven parameters of equation (20).

Acknowledgement

The authors gratefully acknowledge TUBITAK for making this project possible under Grant nos. 104M157 and 108M635.

References

- Boada, M.J.L., Calvo, J.A., Boada, B.L. and Diaz, V. (2008) 'Modeling of a magnetorheological shock absorber by recursive lazy learning', *International Journal of Non-Linear Mechanics*, Article in Press, Corrected Proof, doi:10.1016/j.ijnonlinmec.2008.11.019.
- Chang, C.C. and Roschke, P. (1998) 'Neural network modeling of a magnetorheological shock absorber', *Journal of Intelligent Material Systems and Structures*, Vol. 9, No. 9, pp.755–764.

- Chang, C.C. and Zhou, L. (2002) 'Neural network emulation of inverse dynamics for a magnetorheological shock absorber', *Journal of Structural Engineering*, Vol. 128, No. 2, pp.231–239.
- Choi, S.B., Lee, S.K. and Park, Y.P. (2001) 'A hysteresis model for the field-dependent damping force of a magnetorheological shock absorber', *Journal of Sound and Vibration*, Vol. 245, No. 2, pp.375–383.
- Claudio, C. and Donha, D.C. (2008) 'Discrete-time dynamic model of a magneto-rheological shock absorber for semi-active control design', *ABCMS Symposium Series in Mechatronics*, Vol. 3, pp.27–36.
- Dominguez, A., Sedaghati, R. and Stiharu, I. (2006) 'A new dynamic hysteresis model for magnetorheological shock absorbers', *Smart Material and Structure*, Vol. 15, No. 5, pp.1179–1189.
- Dominguez, A., Sedaghati, R. and Stiharu, I. (2004) 'Modeling the hysteresis phenomenon of magnetorheological shock absorbers', *Smart Material and Structures*, Vol. 13, pp.1351–1361.
- Du, H., Lam, J. and Zhang, N. (2006) 'Modelling of a magneto-rheological shock absorber by evolving radial basis function networks', *Engineering Applications of Artificial Intelligence*, Vol. 19, No. 8, pp.869–881.
- Ehrgott, R.C. and Masri, S.F. (1992) 'Modeling the oscillatory dynamic behavior of electrorheological materials in shear', *Smart Materials and Structures*, Vol. 1, pp.275–285.
- Gamota, D.R. and Filisko, F.E. (1991) 'Dynamic mechanical studies of electrorheological materials: moderate frequencies', *Journal of Rheology*, Vol. 35, pp.399–425.
- Gavin, H., Hoagg, J. and Dobossy, M. (2001) *Optimal Design of MR Shock Absorbers*, US-Japan Workshop on Smart Structures for Improved Seismic Performance in Urban Region, Seattle, WA.
- Gavin, H.P., Hanson, R.D. and Filisko, F.E. (1996) 'Electrorheological shock absorbers, Part II: testing and modeling', *Journal of Applied Mechanics*, Vol. 63, pp.676–682.
- Kim, Y., Langari, R. and Hurlebaus, S. (2009) 'Semiactive nonlinear control of a building with magnetorheological shock absorber system', *Mechanical Systems and Signal Processing*, Vol. 23, pp.300–315.
- Li, W.H., Yao, G.Z., Chen, G., Yeo, S.H. and Yap, F.F. (2000) 'Testing and modeling of a linear MR shock absorber under sinusoidal loading', *Smart Materials and Structures*, Vol. 9, pp.95–102.
- Schurter, K.C. and Roschke, P.N. (2000) 'Fuzzy modeling of a magnetorheological shock absorber using ANFIS', *Proceedings of IEEE International Conference on Fuzzy Systems*, San Antonio, TX, USA, Vol. 1, pp.122–127.
- Spencer, B.F., Dyke, S.J., Sain, M.K. and Carlson, J.D. (1997) 'Phenomenological model of a magnetorheological shock absorber', *Journal of Engineering Mechanics-ASME*, Vol. 123, No. 3, pp.230–238.
- Stanway, R., Sproston, J.L. and Stevens, N.G. (1987) 'Non-linear modelling of an electro-rheological vibration shock absorber', *Journal of Electrostatics*, Vol. 20, No. 2, pp.167–184.
- Wang, D.H. and Liao, W.H. (2004) 'Modeling and control of magnetorheological fluid shock absorbers using neural networks', *Smart Materials and Structures*, Vol. 14, pp.111–126.
- Wen, Y.K. (1976) 'Method of random vibration of hysteretic systems', *Journal of Engineering Mechanics Division- ASCE*, Vol. 102, No. 2, pp.249–263.
- Wereley, N.M., Pang, L. and Kamath, G.M. (1998) 'Idealized hysteresis modeling of electrorheological and magnetorheological shock absorbers', *Journal of Intelligent Material Systems and Structure*, Vol. 9, pp.642–649.
- Wilson, C.M.D. and Abdullah, M. (2005) *Structural Vibration Reduction Using Fuzzy Control of Magnetorheological Shock Absorbers*, ASCE Structures Congress, New York.

- Wong, C.W., Ni, Y.Q., Ko, J.M. (1994) 'Steady-state oscillation of hysteretic differential model ii: performance analysis', *Journal Engineering Mechanical*, Vol. 120, No. 11, pp.2299–2325.
- Yang, G., Jung, H.J. and Spencer Jr., B.F. (2001) *Dynamic Modeling of Full-Scale MR Shock absorbers for Civil Engineering Applications*, US-Japan Workshop on Smart Structures for Improved Seismic Performance in Urban Region, Seattle, WA.
- Yao, B.Z., Yap, F.F., Chen, G., Li, W.H. and Yeo, S.H. (2002) 'MR shock absorber and its application for semi-active control of vehicle suspension system', *Mechatronics*, Vol. 12, pp.963–973.

Nomenclature

τ	Shear stress
τ_y	Dynamic yield stress
H	Magnetic field intensity
du/dr	Shear strain rate
μ	Plastic viscosity
ΔP	Total pressure drop
ΔP_μ	Viscous pressure drop
ΔP_τ	Yield pressure drop
F_μ	Viscous force
F_y	Yield force
Q	Volume flow rate
L	Length of the flow channel
g	Gap of the flow channel
w	Width of the flow channel
c	Coefficient depending on flow velocity
λ	Control ratio
V	Minimum active volume
D	Dynamic range
F_f	Friction force
V_p	Piston velocity
F	Total damping force
Z	Evolutionary variable
$c_0 \dot{x}$	Represents the viscous force
$\alpha, \beta, \gamma, A, c_0, k_0, n$	Characteristic parameters in Bouc-Wen model
$k_0 x$	Linear force due to compressed gas in the accumulator
f_z, az	Evolutionary force
f_{z0}	Evolutionary force at zero velocity
E_t	Error as a function of time
E_x	Error as a function of displacement
$E_{\dot{x}}$	Error as a function of velocity
F_{exp}	Measured force
F_{mod}	Predicted force

All units are SI base units.